

# UC Irvine

## UC Irvine Previously Published Works

### Title

Topical carvedilol delivery prevents UV-induced skin cancer with negligible systemic absorption

### Permalink

<https://escholarship.org/uc/item/5jh1f523>

### Authors

Abdullah Shamim, Md  
Yeung, Steven  
Shahid, Ayaz  
[et al.](#)

### Publication Date

2022

### DOI

10.1016/j.ijpharm.2021.121302

Peer reviewed



Contents lists available at ScienceDirect

International Journal of Pharmaceutics

journal homepage: [www.elsevier.com/locate/ijpharm](http://www.elsevier.com/locate/ijpharm)

## Topical carvedilol delivery prevents UV-induced skin cancer with negligible systemic absorption

Md Abdullah Shamim<sup>a</sup>, Steven Yeung<sup>a</sup>, Ayaz Shahid<sup>a</sup>, Mengbing Chen<sup>a</sup>, Jeffrey Wang<sup>a</sup>, Preshita Desai<sup>a</sup>, Cyrus Parsa<sup>b,c</sup>, Robert Orlando<sup>b,c</sup>, Frank L. Meyskens Jr<sup>d</sup>, Kristen M. Kelly<sup>e</sup>, Bradley T. Andresen<sup>a</sup>, Ying Huang<sup>a,\*</sup>

<sup>a</sup> Department of Pharmaceutical Sciences, College of Pharmacy, Western University of Health Sciences, Pomona, CA, United States

<sup>b</sup> College of Osteopathic Medicine of the Pacific, Western University of Health Sciences, Pomona, CA, United States

<sup>c</sup> Department of Pathology, Beverly Hospital, Montebello, CA, United States

<sup>d</sup> Departments of Medicine and Biological Chemistry, Chao Family Comprehensive Cancer Center, University of California, Irvine, CA, United States

<sup>e</sup> Department of Dermatology, University of California, Irvine, Irvine, CA, United States

### ARTICLE INFO

#### Keywords:

Carvedilol  
Ultraviolet  
Skin cancer  
Chemoprevention  
Transfersome  
Topical delivery

### ABSTRACT

The  $\beta$ -blocker carvedilol prevents ultraviolet (UV)-induced skin cancer, but systemic drug administration may cause unwanted cardiovascular effects. To overcome this limitation, a topical delivery system based on transfersome (T-CAR) was characterized *ex vivo* and *in vivo*. T-CAR was visualized by Transmission Electron Microscopy as nanoparticles of spherical and unilamellar structure. T-CAR incorporated into carbopol gel and in suspension showed similar drug permeation and deposition profiles in Franz diffusion cells loaded with porcine ear skin. In mice exposed to a single dose UV, topical T-CAR gel (10  $\mu$ M) significantly reduced UV-induced skin edema and cyclobutane pyrimidine dimer formation. In mice exposed to chronic UV radiation for 25 weeks, topical T-CAR gel (10  $\mu$ M) significantly delayed the incidence of tumors, reduced tumor number and burden, and attenuated Ki-67 and COX-2 expression. The T-CAR gel was subsequently examined for skin deposition, systemic absorption and cardiovascular effects in mice. In mice treated with repeated doses of T-CAR gel (100  $\mu$ M), the drug was undetectable in plasma, the heart rate was unaffected, but skin deposition was significantly higher than mice treated with oral carvedilol (32 mg/kg/day). These data indicate that the carbopol-based T-CAR gel holds great promise for skin cancer prevention with negligible systemic effects.

### 1. Introduction

Ultraviolet (UV) radiation is a known carcinogen based on evidence from studies in humans and experimental animals (NTP, 2016). Over-exposure to broad-spectrum UV radiation or its components (UVA, UVB, and UVC) causes non-melanoma skin cancer (NMSC) which includes basal-cell and squamous-cell carcinomas (BCC and SCC), as well as melanoma (Ricotti et al., 2009). In contrast to most other tumor types, the NMSC incidence is increasing at an alarming rate in the US and worldwide. In the US, it is estimated that NMSC affects 3 million individuals annually (Guy et al., 2015; Rogers et al., 2015; Siegel et al., 2019). For NMSC, while mortality is lower than some other malignancies, morbidity is very high with millions of people each year requiring surgery or other procedures to prevent progression of lesions which can result in disfigurement, bleeding, infection, and impairment

of essential functions such as vision. Prevention is the best approach to manage NMSC and currently the armamentarium for prevention is very limited and focuses mainly on sun avoidance or protection via commercially available sun block lotions.

The  $\beta$ -blocker carvedilol, an FDA approved oral drug used to manage cardiovascular disorders such as hypertension and heart failure, has shown promising activity in the prevention of UV-induced skin DNA damage and carcinogenesis (Chang et al., 2015; Huang et al., 2017a). The anticancer mechanism for carvedilol likely involves a multifunctional action including inhibition of UV-induced DNA damage, inflammation, and oncogenic signaling pathways such as PI3K/AKT, MAPK/ERK, AP-1, COX-2 and NF- $\kappa$ B (Chen et al., 2020a; Cleveland et al., 2018; Huang et al., 2017b; Ma et al., 2019). Consistent with the preclinical activity of carvedilol in cancer prevention, a population-based cohort study of 6,771 individuals demonstrated that long-term use of carvedilol

\* Corresponding author at: Western University of Health Sciences, 309 E. 2<sup>nd</sup> St., Pomona, CA 91766, United States.

E-mail address: [yhuang@westernu.edu](mailto:yhuang@westernu.edu) (Y. Huang).

<https://doi.org/10.1016/j.ijpharm.2021.121302>

Received 21 August 2021; Received in revised form 8 November 2021; Accepted 11 November 2021

Available online 15 November 2021

0378-5173/© 2021 Elsevier B.V. All rights reserved.

was associated with a reduced risk of all types of cancer examined (Lin et al., 2015). A second clinical study examining women taking carvedilol prior to breast cancer diagnosis demonstrated reduced breast cancer mortality (Gillis et al., 2021). In both cases, the patients were prescribed carvedilol to treat cardiovascular diseases.

There are challenges in repurposing carvedilol as a cancer preventive treatment. Foremost, as a highly potent  $\beta$ -blocker ( $IC_{50} \sim 1$  nM (Yao et al., 2003)), carvedilol shows cardiovascular effects, namely bradycardia and hypotension, which are undesirable in patients without cardiovascular diseases. Secondly, due to a significant degree of first-pass metabolism, the bioavailability for oral carvedilol is only 24% (von Mollendorff et al., 1987), therefore high dosing frequency is needed to obtain pharmacological effects. Topical drug delivery offers a solution to the challenges of repurposing carvedilol as a cancer preventive treatment. Firstly, targeting carvedilol to the skin allows for local delivery and should reduce systemic effects; thereby, limiting the likelihood of unwanted cardiovascular effects. Secondly, directly targeting the skin avoids the first-pass effect, and should allow for increased concentration of carvedilol only at the desired site of action.

In this context, various nanoformulation strategies have been reported in the literature to achieve the desired skin targeting. Among these, we rationalised to formulate nano-transfersomes of carvedilol because of their unique vesicular structure, flexibility and elasticity that allow deep skin penetration (Opatha et al., 2020; Sana et al., 2021). In our previous study, we reported detailed development and characterization of a carvedilol loaded nano-transfersome for skin-targeted drug delivery (Chen et al., 2020b). In vitro skin penetration and retention studies using Franz diffusion cells and porcine ear skin demonstrated that the transfersome was effective in delivering the drug into the skin layers and produced a controlled and prolonged skin delivery of drug (Chen et al., 2020b). Furthermore, the carvedilol loaded transfersome suppressed UV-induced DNA damage, inflammatory gene expression, and apoptosis on reconstructed full-thickness human skin culture.

In the present study, the carvedilol loaded transfersome, given the name T-CAR, was further characterized in vivo. To facilitate topical application to mice, T-CAR was prepared as a carbopol-based gel. The T-CAR gel was first tested to ensure that the gel did not alter skin deposition of drug, nor the skin cancer preventative properties of carvedilol. Additionally, pharmacokinetic and cardiovascular studies were conducted to determine if the drug is found in the systemic circulation and causes cardiovascular effects. The hypotheses tested is that 1) The T-CAR gel is effective in preventing UV-induced skin damage and tumor development, and 2) The T-CAR gel does not facilitate systemic delivery of carvedilol and thus does not alter mouse heart rate. The data obtained demonstrated the feasibility for the use of transfersome as a topical delivery system for carvedilol, allowing for carvedilol to be repurposed for skin cancer chemoprevention.

## 2. Materials and methods

### 2.1. Compounds and materials

Carvedilol was purchased from TCI America (Portland, OR). Tween-80, Polyethylene glycol 400 (PEG 400), methanol, chloroform and phosphate-buffered saline (PBS) tablets were purchased from VWR (Radnor, PA). L- $\alpha$ -phosphatidylcholine (Soy PC or SPC) was purchased from Avanti Polar Lipids, Inc. (Alabaster, AL). Isoproterenol was purchased from Tocris (Minneapolis, MN). Carbopol 934 was purchased from SERVA Electrophoresis GmbH (Heidelberg, Germany). Triethanolamine (TEA) was purchased from Sigma-Aldrich.

### 2.2. Preparation of carvedilol loaded transfersome (T-CAR) and carbopol-based gel

T-CAR were prepared by a thin film hydration method as described previously with slight modification (Chen et al., 2020b). The empty

transfersome was prepared identically except no carvedilol was added. Gel formulations were prepared according to a published study (Bhatia et al., 2012). Briefly, 0.5% Carbopol dispersion was prepared in nanopure water. T-CAR suspension and the neutralizer TEA (1:1.5 ratio of Carbopol: TEA, w/w) were then added and vortexed until forming clear gel formulation.

### 2.3. Determination of particle size, polydispersity index (PDI), zeta potential and encapsulation efficiency (EE)

The particle size and PDI for T-CAR (undiluted sample) were analyzed via a Nanobrook Omni particle sizer (Brookhaven Instruments Corporation, Holtsville, NY), and zeta potential determined with a Malvern zeta-sizer (Malvern Panalytical, Malvern, United Kingdom). For EE, the transfersomes were centrifuged in 30,000-dalton cutoff Nanosep® tubes (Pall Life Sciences, Ann Arbor, MI) at 14,000 rpm for 1 h at 4 °C. The EE was determined according to previously reported methods (Chen et al., 2020b).

### 2.4. Transmission electron microscopic (TEM) analysis

TEM is a visualization tool for directly imaging nanoparticles to obtain a quantitative measure of particle size, size distribution, and morphology (Mahmood et al., 2014). The T-CAR was examined by TEM with the negative staining method by nanoComposix (San Diego, CA). In brief, samples were prepared for imaging by drying the nanoparticles on a copper grid coated with a thin layer of carbon. Images were obtained by the use of a transmission electron microscope operating at an accelerating voltage of 100 keV and an AMT XR41-B 4-megapixel (2048 × 2048) bottom mount CCD camera. The camera's finite-conjugate optical coupler provides high resolution and flat focus with <0.1% distortion for magnifications as high as 150,000x.

### 2.5. Ex vivo skin permeation study

The ex vivo skin permeation studies were performed according to reported methods (Chen et al., 2020b). In brief, the Franz diffusion system (Crown Glass Company, Somerville, NJ, USA) with a surface area of 1.13 cm<sup>2</sup> was mounted with porcine ear skin (Sierra for Medical Science, Whittier, CA) as a model for human skin. The receptor compartment was filled with 5.5 mL of 40% v/v PEG 400 in PBS (pH 7.4) (PEG 400 was added to increase the solubility of permeated carvedilol) and maintained at 37 °C under magnetic stirring. 0.2 mL of T-CAR suspension or the same volume of gel containing 4  $\mu$ g carvedilol was applied to the porcine skin in the donor compartment. At predetermined time intervals (0.5, 1, 2, 3, 4, 6, 20, 24, 48, and 72 h), 0.2 mL solvent in the receptor compartment was collected and replaced with 0.2 mL solvent. The drug content in the samples was analyzed by HPLC, and the concentration was corrected for sampling effects according to reported methods (Gannu et al., 2008).

### 2.6. Tape-stripping

To analyze the drug penetration into the skin layers, a tape-stripping method was used according to previous reports (Chen et al., 2020b; Freitas et al., 2015; Lademann et al., 2009). After removing the stratum corneum, the remaining layers consisting of the epidermis and dermis were collected in 400  $\mu$ L of PBS for homogenization. The samples were then mechanically shaken for one hour by adding 600  $\mu$ L of methanol. After centrifuging for 10 min at 10,000 rpm, the supernatant was collected and analyzed by HPLC.

### 2.7. HPLC analysis

HPLC analysis was performed using an Agilent 1260 HPLC system (Agilent Technologies Inc., Santa Clara, CA, US) for the determination of

carvedilol levels, with methods reported previously (Chen et al., 2020b).

## 2.8. LC/MS/MS analysis

The LC/MS/MS system consists of an API3200 LC/MS/MS system (Sciex, Framingham, MA), two Shimadzu LC-20AD Prominence HPLC pumps equipped with an SIL-20A Prominence autosampler (Shimadzu, Columbia, MD) and the Analyst 1.5.1 software. Carvedilol was separated on a BDS Hypersil C18 reverse-phase column (2.1 × 150 mm; 5 μm) together with a C18 guard column (2.1 × 10 mm, 5 μm) at room temperature. The mobile phase was (A) 2 mM ammonium acetate containing 0.1% formic acid and (B) acetonitrile. The following linear gradient at a flow rate of 0.3 mL/min was used: an initial condition of 20% eluent B kept constant for 1 min; increasing linearly to 75% eluent B over 0.5 min; remaining at 75% B for 4 min; lowering to 20% over 0.5 min; and reconditioning for 2 min. The total run time was 8 min. The optimization of mass spectrometric parameters was conducted by infusing the standard solution of each analyte (100 ng/ml) at a flow rate of 5 μL/min, which were prepared in 0.1% formic acid:acetonitrile (1:1). The protonated ions of carvedilol (407.138) and propranolol (260.145) (internal standard) were detected using the positive ESI mode. The MS conditions were optimized using Compound Optimization module built into the Analyst software. The most abundant product ions of 224.2 and 116.058 *m/z* were selected for carvedilol and propranolol, respectively. The mass spectrometric conditions used: curtain gas, 25 psi; collision gas, 5; ion spray voltage, 5500 eV; temperature, 550 °C, gas 1, nitrogen, 40 psi; gas 2, nitrogen, 20 psi. The detection limit of carvedilol by this method is 2 ng/mL.

## 2.9. Acute UV exposure of mice

All animal studies were carried out under the recommendations and guidelines established by Western University of Health Sciences' Institutional Animal Care and Use Committees which approved these studies. Mice had access to water and food ad libitum and housed on a 12-hour light/dark cycle with 35% humidity. All mice were obtained from our internal breeding protocol. Female SKH-1 hairless mice, seven-eight week of age, were randomly divided into five groups (n = 5): (1) no UV negative control, (2) UV + acetone, (3) UV + 10 μM carvedilol in acetone (10 μM or 4 μg/mL, 0.8 μg per treatment), (4) UV + empty transfersomes gel formulation, and (5) UV + T-CAR gel formulation. The UV lamps used in these studies were described before (Liang et al., 2021). A half-hour prior to UV-radiation, the mice were pre-treated with different treatments as described above. For acetone or carvedilol in acetone groups, 200 μL volume of acetone was applied to the back of mouse. For T-CAR gel group, 200 μL gel formulation containing same amount of carvedilol as group 3 was applied to the back of mouse. For the empty transfersome gel formulation group, formulation containing the same amount of gel was applied to each mouse. The area of treatment for each mouse was approximately 6 cm<sup>2</sup> of back skin. The mice were then radiated with UV at a dose of 224 mJ/cm<sup>2</sup>. During the UV exposure, mice roamed freely in acrylic cages on a rotating platform with rotational placement ensuring consistent and equal dorsal distribution of UV irradiation. Immediately after UV radiation, all groups were administered again with the same treatments. Six hours after UV exposure, all mice were euthanized. Whole skin samples and plasma were collected for further investigations.

## 2.10. Chronic UV-induced skin tumorigenesis

Seven-eight week-old female SKH-1 mice were randomly divided into three groups (n = 10): (1) UV-treated control, (2) UV-exposed followed by empty transfersome treatment, and (3) UV-exposed followed by T-CAR treatment (10 μM of drug). The volume for topical treatment was 200 μL for both empty transfersome and T-CAR, and after week 19, due to larger body size of mice, the dose was increased to 300 μL. Mice

were pretreated with T-CAR and empty transfersomes three times a week for two weeks before starting UV exposure. The UV treatment protocol was described before (Liang et al., 2021). In brief, the mice were irradiated with gradually increasing levels of UV three times a week for 25 weeks with an initial dose of 50 mJ/cm<sup>2</sup> that was increased each week by 25 mJ/cm<sup>2</sup> to 150 mJ/cm<sup>2</sup>, which was continued for the duration of the experiment. The drug was applied topically immediately after each radiation throughout the course of the experiment. Tumors of at least 1 mm in diameter were counted and measured with a Caliper weekly. The tumor volume was calculated according to the formula: (width)<sup>2</sup> × length/2. Mouse photo was taken weekly. At the end of the 25th week, mice were euthanized, and tumorous and non-tumorous skin samples were excised and fixed in 10% formalin for histological analysis.

## 2.11. Cyclobutane pyrimidine dimer (CPD) dot blot analysis

CPD assay was performed according to published protocol (Park and Kang, 2015). In brief, genomic DNA was isolated from dorsal skin samples by QIAamp DNA Mini Kit (Qiagen, Germantown, MD). The denatured DNA samples (100 ng) were vacuum-transferred to a nitrocellulose membrane (0.45 μm, Thermo Scientific) using a Bio-Dot SF microfiltration apparatus (Bio-Rad, Hercules, CA). CPDs were detected by immunoslot blot using anti-CPD monoclonal antibody (Kamiya, Seattle, WA). After the immunoslot blot assay, total DNA amounts loaded onto the membrane were determined by anti-DNA antibodies, single-stranded, clone 16–19 (Sigma), and these values were used to normalize the CPD values.

## 2.12. Histology and Immunohistochemistry (IHC) analysis

The skin tissues or tumors were fixed in formalin, processed, and embedded in paraffin blocks. 5 μm-thick prepared sections of the paraffin-embedded skin tissues were placed onto positively charged glass slides. The sections were stained with hematoxylin and eosin (H&E). The protocol for IHC was described in previous publication (Liang et al., 2021). The antibodies used are anti-COX-2 (1:600, Cell Signaling Technology, Danvers, MA, Cat no. 12282) and Ki-67 (1:400, Cell Signaling Technology, Cat no. 12202). The slides were imaged with a microscope at 20x or 40x magnification (Leica DM750, Buffalo Grove, IL). Ki-67 was scored by counting the positively stained cells in five fields at various locations along the skin section to obtain the average for each mouse skin (n = 3 mice for short term UV study; n = 3 ~ 5 mice for long term UV study). For the extent of staining of COX-2, the following system was used: 0, no staining, 1 is < 25% of cells positive, 2 is > 25% and ≤ 50% of cells positive, and 3 is > 50% of cells positive. For staining intensity, the following system was used: 0 is no staining, 1 is faint staining, 2 is moderate staining, and 3 is strong staining. To quantitate COX-2 staining, an expression index was calculated by extent of staining multiplied by the intensity of staining.

## 2.13. Pharmacokinetic analysis of topically applied T-CAR or oral carvedilol

Forty-five male SKH-1 mice (seven-week of age) were randomly divided into the following three groups (15 mice per group): (1) oral administration of 20 mg/kg of carvedilol by gavage, (2) topical administration of 10 μM carvedilol in acetone (200 μL), and (3) topical administration of T-CAR gel formulation containing 10 μM carvedilol (200 μL). All mice were administered with a single dose of treatments. The mice were euthanized at 0.5, 2, 4, 6 and 8 h after treatment (n = 3 per group for each time point). Blood samples were collected from the heart and placed into heparinized Eppendorf tubes and immediately centrifuged. Separated plasma was collected for LC/MS/MS analysis.

#### 2.14. Cardiovascular effects of topically applied T-CAR or oral carvedilol

Cardiovascular parameters were collected non-invasively using a volume-pressure recording (VPR) tail-cuff method on conscious mice using the CODA 8-Channel High Throughput system (Kent Scientific Corp, Torrington, CT). Sixteen mice were randomly divided into two groups: (1) orally administered carvedilol and (2) topically applied carvedilol-loaded transfersome. To minimize variation, the tail temperature was maintained between 32°C to 35°C, the animals were covered to retain warmth and to calm the mice. Each mouse was allowed to rest for 15 min within the restraint chamber before recordings were performed with five acclimation cycles, 10 test cycles, 5 s between cycles, a deflation time of 15 s, a maximum occlusion pressure of 250 mmHg, and a minimum volume of 15  $\mu$ L. The resulting systolic blood pressure (SBP), diastolic blood pressure (DBP), mean blood pressure (MBP), and heart rate (HR) were collected and averaged to obtain a single value from each run. Tail cuff measurements require an acclimation period as the stress of restraint can induce a sympathetic response. In a pilot study with SKH-1 mice, we found that two weeks acclimation produced data that had a coefficient of variation (CV) of <10% in 78% of the animals tested, and further acclimation did not significantly change the CV. Therefore, a two-week acclimation period of measuring twice a week (Mondays and Thursdays) was conducted prior to beginning of the experiment. The mean heart rate, our primary endpoint, had a 9% CV on the last acclimation day. Following acclimation, heart rate and blood pressure were measured at the same interval for two weeks to establish baseline parameters. At the end of the baseline measurements, the isoproterenol (Iso)-loaded mini-pumps were inserted into the mice. The pumps were inserted subcutaneously into each individual mouse initiating a two-week Iso treatment paradigm. Iso is a  $\beta$ 1- and  $\beta$ 2-adrenergic receptor agonist, that increases heart rate and contractility as well as peripheral vasodilation, and the physiological effects of Iso are attenuated by  $\beta$ -blockers (Zhang et al., 2005). Briefly, 100  $\mu$ L Iso was loaded into Alzet (Cupertino, CA, US) micro-osmotic pumps model 1004 to deliver 20  $\mu$ g/kg/day, according to published protocol (Chang et al., 2018). Assuming the body weight for mouse is 25 g, the total drug given to each mouse will be 0.5  $\mu$ g per day. The pump we used is 0.11  $\mu$ L/hr = 2.64  $\mu$ L/day and therefore, the drug concentration in each pump was 0.19  $\mu$ g/ $\mu$ L. Following the two-week Iso treatment, carvedilol treatment was initiated. Carvedilol was dissolved in drinking water for an estimated dose of 32 mg/kg/day for group 1, and 300  $\mu$ L of T-CAR gel was applied topically daily for two weeks at a concentration of 100  $\mu$ M in group 2. The oral delivery of carvedilol was based previous report (Wang et al., 2011). In brief, a 25 g mouse would need to take 0.799 mg per day to achieve 32 mg/kg body weight/day. Typically, a 25 g mouse drinks 4.5 mL liquid per day, therefore, the drug will be diluted in the drinking water to a concentration of 0.178 mg/mL. Animals under treatment were provided ad libitum access to testing drug-infused water as the sole source of drinking fluid. Twenty-four hours following the last topical treatment, plasma and skin samples were collected to determine the amount of carvedilol via LC/MS/MS.

#### 2.15. Statistical analysis

All the data were expressed as a mean  $\pm$  standard deviation (SD), standard error (SE), or 95% confidence interval, as stated with the data presentation, with a line representing the group mean. The specific error shown is described in the figure legend. All plots were made using GraphPad Prism version 9.0 (La Jolla, CA, USA). The specific statistical tests are detailed in the text and figure legends. Tumor data were graphed using a Kaplan-Meier survival curve showing the incidence of tumors forming in GraphPad Prism and analyzed using a Mantel-Cox log-rank test. Total tumor volume and tumor multiplicity was analyzed by repeated measured ANOVA followed by Tukey-Kramer post hoc tests. The Grubbs' outlier test based on the extreme studentized deviate method, was used to determine whether an extreme value in

tumor volume is a significant outlier at the Significance level  $\alpha = 0.05$  (two-sided). Differences in tumor severity was tested via a Chi-square analysis of all groups and then individual tests to identify which groups are statistically different from each other. For all statistical analyses, means were indicated to be statistically different when  $p < 0.05$ .

### 3. Results

#### 3.1. Characterization of transfersomes

During formulation development, three batches of T-CAR and two batches of empty transfersomes have been made. **Supplementary Table 1** shows the data of particle size, PDI, zeta potential and EE. For T-CAR, the average particle size was  $88.89 \pm 6.64$  nm, the average zeta potential was  $34.72 \pm 3.04$  mV, and the average EE was  $95.1 \pm 1.19\%$ . The batches were found to be consistent with uniform size distribution which was confirmed with low PDI of  $0.116 \pm 0.041$ . **Fig. 1A** shows the particle size distribution for T-CAR and the empty transfersomes (batch #1) based on the Dynamic Light Scattering (DLS) method. The size of T-CAR was slightly smaller than previously reported data (Chen et al., 2020b) possibly because undiluted samples were used for the measurement in the present study.

TEM analysis was used to confirm the DLS data and examine the morphology of T-CAR. TEM allows the imaging of the transfersomes in their original form without sample modification such as labeling or fixation (Mahmood et al., 2014). From the representative TEM micrographs (**Fig. 1B**), circular unilamellar lipid vesicles can be observed. Some irregularly shaped particles are observed, possible due to the quick drying of the transfersome during the staining process. About 35% of the particles were around 100 nm (**Fig. 1C**) which is consistent with the DLS data (**Fig. 1A**).

#### 3.2. Ex vivo skin drug permeation study of T-CAR gel

To facilitate topical application, a 0.5% Carbopol® 934 gel dispersion for T-CAR was prepared (**Fig. 2A**). To ensure the carvedilol loaded transfersome in gel or in suspension similarly permeate the skin, the Franz diffusion cell system was used. For studies of skin drug penetration, porcine ear skin shows similarities in histology and structure including hair follicles compared with human skin (Jacobi et al., 2007) and therefore was used as a surrogate for human skin. The percentage cumulative carvedilol permeated at various time points for gel or suspension forms of T-CAR is shown in **Fig. 2B**. For both T-CAR suspension and gel, the drug was not detectable within the first 4 h. From the 6-hour time point, the skin penetration of T-CAR increased until gradually plateauing after 24 h. Across all the time points studied, the cumulative drug permeated through the pig ear skin showed a similar profile for the gel form and the suspension form. **Supplementary Fig. 1** shows the comparison of drug permeation profiles of free drug in acetone, T-CAR suspension, and T-CAR gel. Although the T-CAR gel shows the trend of slower permeation, there was no significant difference between the three groups. To verify the ex vivo data, the drug release profiles in vitro for the three formulations containing 0.1 mg carvedilol were compared (**Supplementary Fig. 2**). As expected, T-CAR suspension and gel showed much slower drug release profile than the free drug in acetone, while the release profiles for suspension and gel were similar. The experiment was repeated and at 24 h the skin was collected, and tape-stripped to analyze the carvedilol in the epidermis and dermis (**Fig. 2C**). For the T-CAR suspension a  $38.91 \pm 7.74\%$  (mean  $\pm$  SD) was detected in the stripped skin, while for T-CAR gel,  $30.88 \pm 8.7\%$  (mean  $\pm$  SD) was in the stripped skin. Although T-CAR gel produced slightly lower skin retention, no statistical difference was detected between the two groups. The delayed and slow transdermal permeation plateauing after 24 h coupled with significant carvedilol epidermal-dermal skin retention confirmed the hypotheses of deep skin penetration with transfersomes which is important for topical prevention of UV-induced skin cancer.

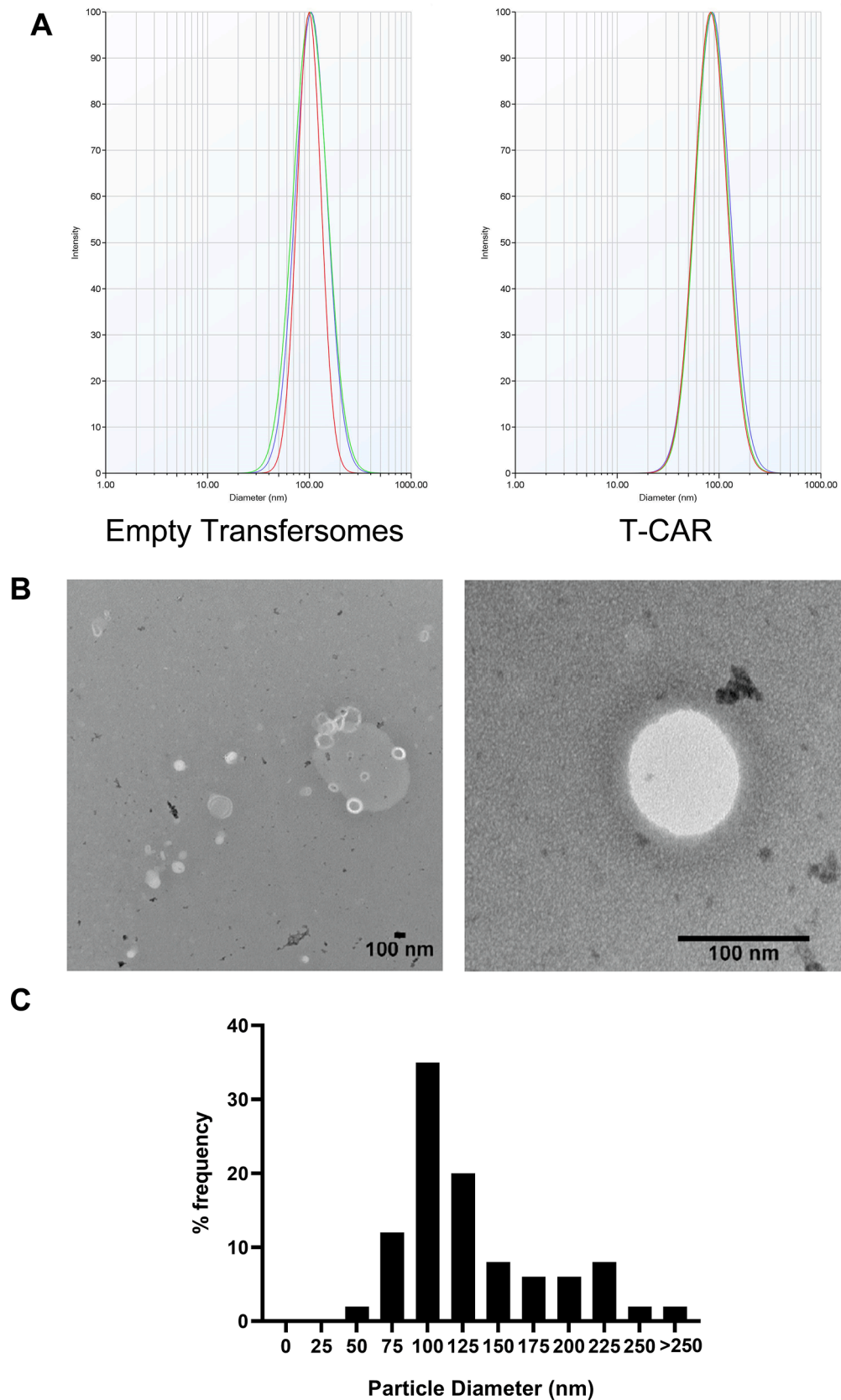


**Fig. 1.** Transfersome size and Transmission electron microscopy (TEM) analysis. (A) Representative transfersome size distribution by Malvern particle size analyzer for empty transfersome and T-CAR (batch #1). (B) Representative TEM photomicrographs of T-CAR. The scale bar represents 100 nm. (C) The particle size and distributions in frequency (%) for T-CAR derived from the TEM analysis.

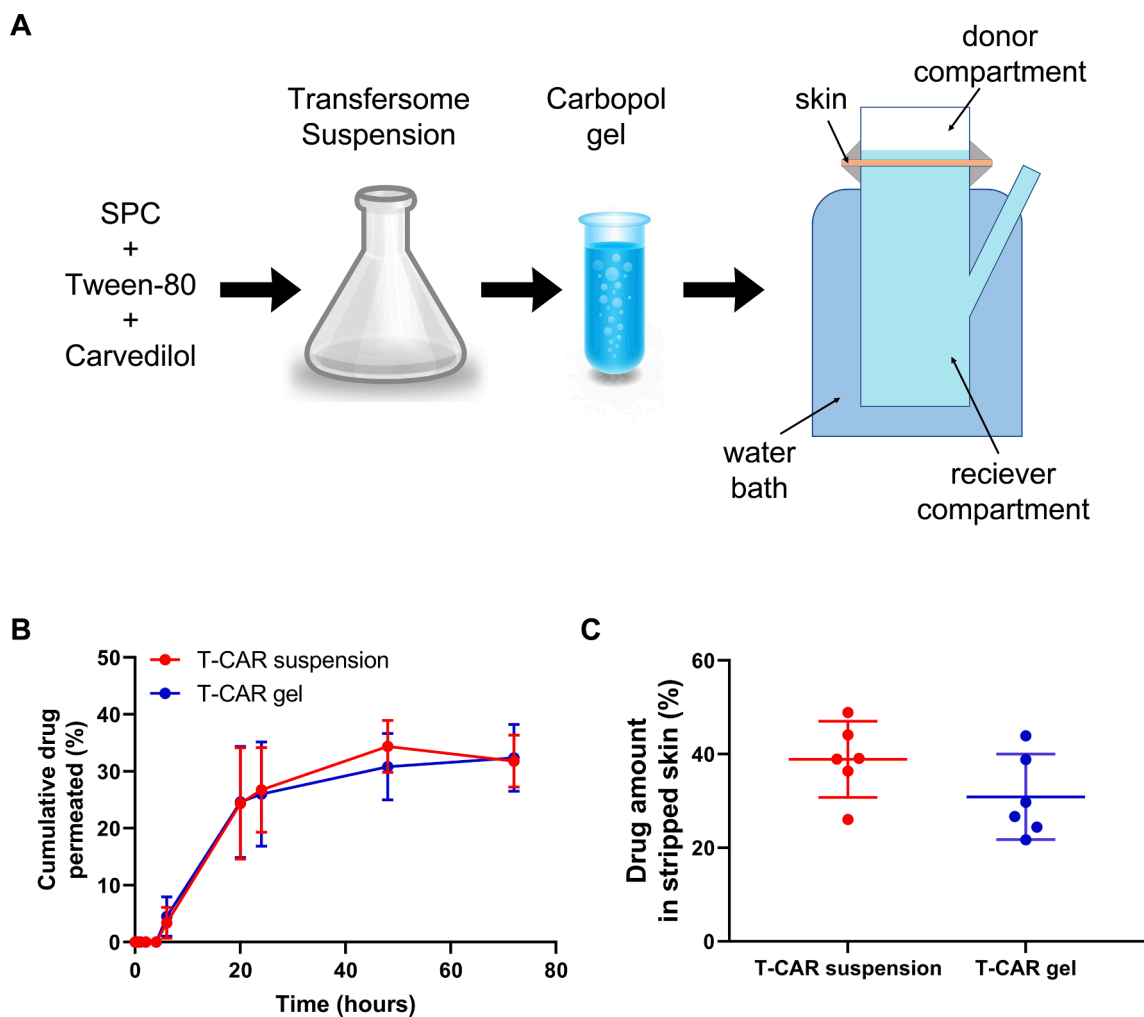


**Fig. 2.** Ex vivo skin drug permeation profiles of T-CAR in suspension or in gel. (A) A flow chart of making T-CAR carbopol gel. T-CAR (each containing 4.0  $\mu$ g carvedilol, 0.2 mL) was added to the donor compartment of a Franz diffusion device. 0.2 mL release media was withdrawn from receiver compartment at predesigned time points for HPLC analysis. (B) Cumulative carvedilol permeated into the receptor compartment as a function of time up to 72 h. The receiver compartment contains PBS containing 40% v/v of PEG400. Data are presented as mean  $\pm$  SD (n = 3). (C) Carvedilol levels in stripped skin (epidermal and dermal layers) 24 h after loading the drugs, determined via HPLC. Data are presented as mean  $\pm$  95% CI. (n = 6).

### 3.3. Effects of T-CAR on acute UV-induced skin damage in mice

In order to determine the pharmacological effects of T-CAR, SKH-1 hairless mice were administered with free carvedilol, T-CAR, or the respective vehicle controls and irradiated with a single dose UV (224  $\text{mJ}/\text{cm}^2$ ) and the treatment was immediately re-administered. Six hours after UV exposure, the dorsal skin was collected for H&E staining (to quantify epidermal thickening) and cyclobutene pyrimidine dimer (CPD) formation (the DNA damage marker). The H&E images showed that the epidermis was significantly thicker in UV control group treated with vehicle or the empty transfersome group than the “no UV” negative control group (Fig. 3A & B). Topical administration of free carvedilol dissolved in acetone and T-CAR gel formulation statistically attenuated UV-induced skin thickening in a similar manner (Fig. 3B). Since UV exposure induces CPD formation, DNA was extracted from whole dorsal skin tissue and denatured to evaluate the CPD levels. UV exposure induced CPD formation in SKH-1 mice skin (Fig. 3C). Paralleling the skin thickening data, topical administration of free carvedilol dissolved in acetone (CAR) and T-CAR gel formulation statistically attenuated CPD formation (Fig. 3D). These data suggest that in terms of skin damage protection, the T-CAR gel formulation is as effective as the free carvedilol dissolved in acetone.

### 3.4. Effects of topically applied T-CAR on chronic UV-induced skin carcinogenesis in mice

Previous data demonstrated that topically applied free carvedilol dissolved in acetone (10  $\mu\text{M}$ ) statistically delays UV-induced skin carcinogenesis in mice (Huang et al., 2017b). However, acetone is not an appropriate vehicle for delivering drugs to humans. Therefore, T-CAR gel and empty transfersomes gel was tested for chemopreventive properties in an identical assay as previously conducted for carvedilol in acetone. The mice were pre-treated for two weeks, then irradiated by gradually increasing levels of UV radiation from 50  $\text{mJ}/\text{cm}^2$  to 150  $\text{mJ}/\text{cm}^2$  three times a week for 25 weeks to induce skin tumors as reported previously (Huang et al., 2017b). The drug treatment was applied immediately after each UV exposure to avoid sunscreen effects. At week 16, tumors appeared in all three groups. However, Cox Regression analysis indicates that T-CAR statistically slows the incidence of UV-induced tumors ( $p = 0.0379$ ) whereas the empty transfersome treatment did not statistically differ from the UV control group (Fig. 4A). The median tumor incidence is four weeks longer when treated with T-CAR gel, which is statistically different than the UV control and empty transfersomes (Table 1). Not surprisingly, the delayed median incidence of T-CAR gel treatment is associated with fewer total tumors and fewer tumors per mouse (Table 1). Similarly, total tumor volume per mouse is

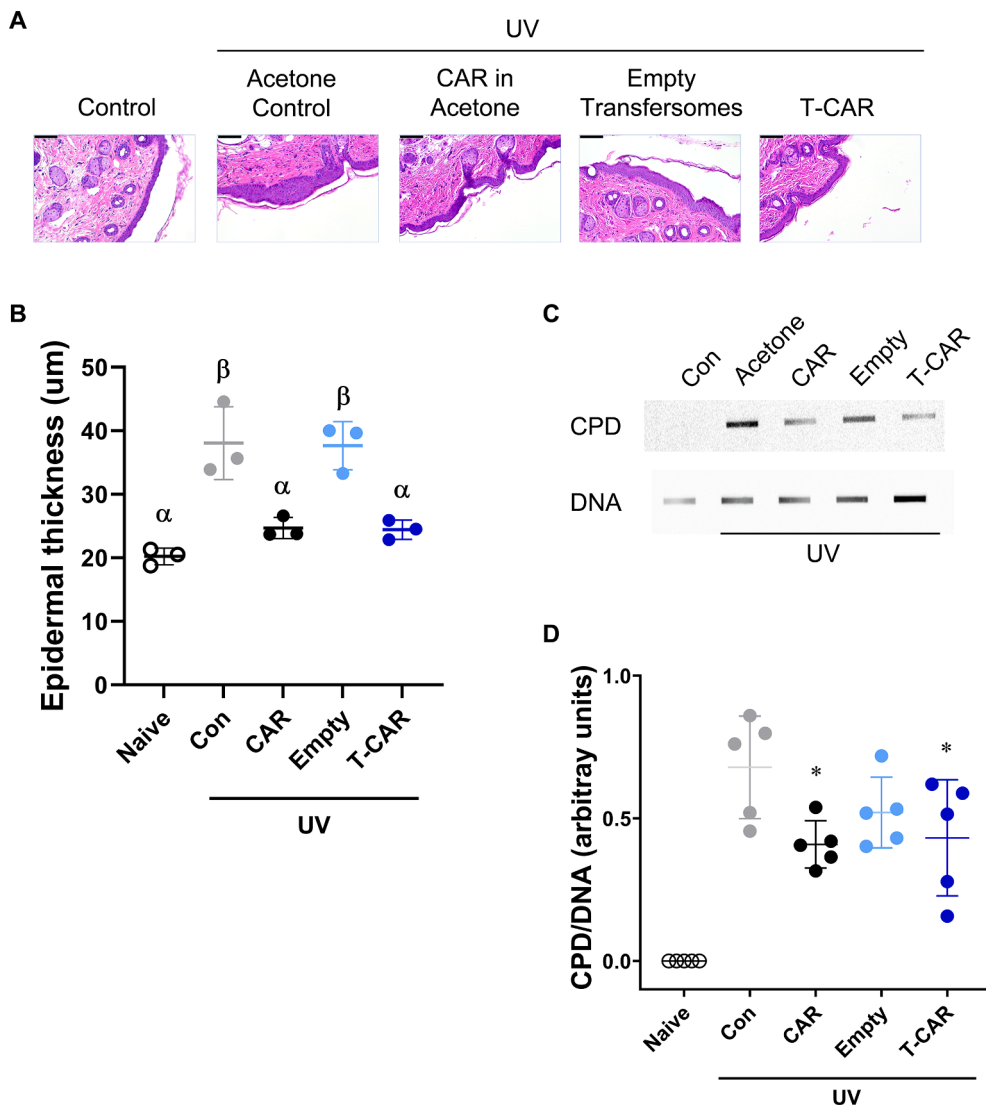


**Fig. 3.** Effects of T-CAR on acute UV-induced skin damage. SKH-1 mice were treated with 10  $\mu$ M carvedilol in acetone, 10  $\mu$ M T-CAR, acetone, or empty transfersome then irradiated with 224 mJ/cm<sup>2</sup> of UV and the treatments reapplied; a non-treated control was included. (A) Representative H&E staining of the control and treated mouse skin (scale bar is 100 nm), and (B) measurement of epidermal thickness. Groups with different Greek letters are statistically different ( $P < 0.05$ ), as determined by ANOVA followed by Tukey-Kramer post hoc test. (C) Slot blot assay for CPD. Each band represents DNA from one mouse from each treatment group. Genomic DNA was isolated from the dorsal skin of mice. (D) CPD data was expressed as mean  $\pm$  SD;  $n = 5$ . Groups with an asterisk symbol are statistically different ( $P < 0.05$ ) than UV control as determined by ANOVA followed by a Dunnett's 2-Sided test.

different between the groups as per an RM-ANOVA ( $p = 0.022115$ ), and, expectedly, time is a significant contributor to tumor growth ( $p = 0.000000$ ). There is also a statistical interaction between the treatment group and time ( $p = 0.000131$ ); however, only T-CAR gel treatment statistically reduces mean tumor volume from UV-treated animals as per a Tukey-Kramer post hoc test. Although there is a statistical difference in tumor volume, there is no difference in doubling time (Table 1) indicating that once a tumor is established T-CAR has no effect, and the observed difference is due to the delay in tumor formation. Thus, consistent with the data obtained with free drug (Huang et al., 2017b), the T-CAR gel formulation effectively allows for carvedilol-mediated skin cancer prevention.

From each of the three treatment groups, eight selected tumors with the largest volume in each group were dissected for histological analysis. In the UV only group, 4 of the 8 tumors were diagnosed as invasive SCC, the remaining are premalignant papillomas. In empty transfersomal group, 2 of the 8 tumors are invasive SCC, the remaining are premalignant papillomas. However, in the T-CAR group, all the 8 tumors are benign papilloma. Representative H & E images are shown in Fig. 4B. A Chi-square analysis indicates that the distribution of tumors in the three groups is statistically different ( $\chi^2$  of 25.6,  $df = 4$ ,  $p < 0.0001$ ), with T-CAR being the only treatment different than the UV control ( $\chi^2$  of 16.0,  $df = 2$ ,  $p = 0.0003$ ), and also the empty transfersomes ( $\chi^2$  of 16.0,  $df = 2$ ,  $p = 0.0003$ ).

Non-cancerous skin sections dissected from tumor-bearing mice treated with T-CAR gel showed significantly reduced epidermal hyperplasia compared to UV treated mice, whereas gel containing empty transfersomes had no significant effect (Fig. 5A). Similar differences were found for Ki-67 and COX-2 staining in non-cancerous skin sections (Fig. 5B&C). T-CAR, but not empty transfersome, statistically reduced Ki-67 positive cells in each mouse (Fig. 5B), and the intensity of COX-2 staining (Fig. 5C). Thus, the long-term UV carcinogenesis studies confirm the chemopreventive activity of the T-CAR gel formulation.

### 3.5. Pharmacokinetic and heart rate analysis of T-CAR in mice

The pharmacokinetic properties of a single dose topically applied T-CAR gel (10  $\mu$ M drug), which contains identical drug concentrations in T-CAR used in the in vivo studies (Figs. 3-5), was compared with 10  $\mu$ M free carvedilol in acetone and with a positive control - a single oral dose of carvedilol (20 mg/kg). Fig. 6A shows the blood plasma levels of carvedilol beginning 30 min after carvedilol administration. Oral gavage resulted in rapid absorption and reached a peak concentration within 1 to 2 h, and has an elimination half-life of 4 to 7 h. However, the results indicate that at no time after the single topical treatment of T-CAR gel or free carvedilol in acetone was there a detectable plasma concentration of carvedilol. Therefore, single topical application of 10  $\mu$ M T-CAR and free carvedilol does not result in noticeable plasma concentrations within



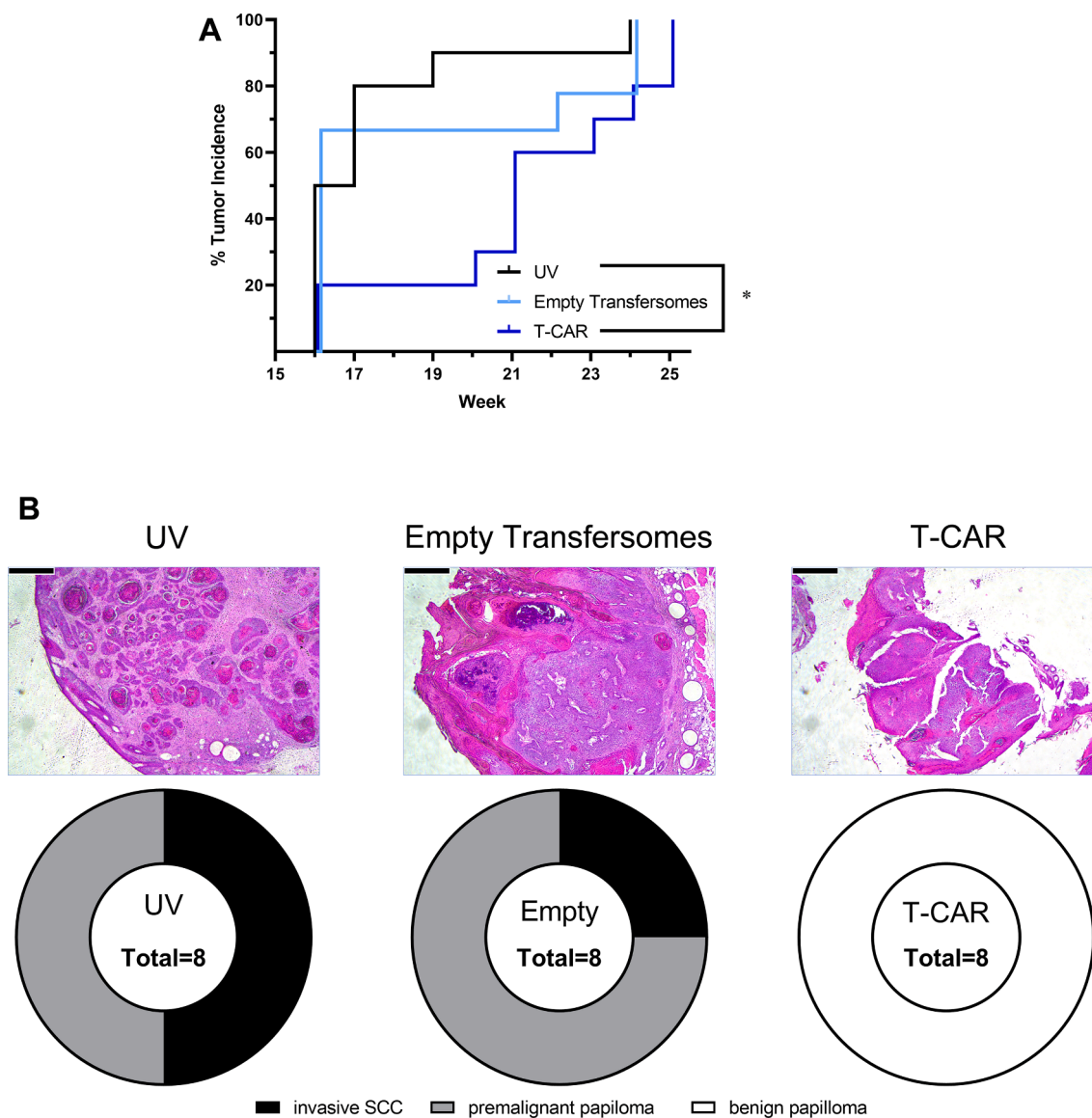


**Fig. 4.** Effects of T-CAR gel on the development of UV-induced skin tumors in SKH-1 mice. Mice were pre-treated with the T-CAR gel or empty transfersome for two weeks. The mice were then exposed to gradual doses of UV up to 150 mJ/cm<sup>2</sup> three times per week, and drug treatments were given immediately after each irradiation. (A) Tumor incidence is graphed as a Kaplan-Meier curve and analyzed via a Mantel-Cox log-rank test. Groups that are statistically different ( $p < 0.05$ ) are denoted with an asterisk (\*) in the legend;  $n = 10$ . (B) From each group, eight tumors with the largest volume were dissected for histological analysis, showing SCC, papilloma and epidermal dysplasia in various distribution.

eight hours.

Multiple doses of a drug can increase plasma concentrations beyond a single dose and should result in a steady state of carvedilol exposure. Since carvedilol is a  $\beta$ -blocker that decreases heart rate and blood pressure (Hanada et al., 2008), we examined the heart rate of SKH-1 mice which were orally administered carvedilol or topically applied T-CAR gel. Baseline heart rate was measured for two weeks. Then a 28-day micro-osmotic pump delivering 20  $\mu$ g/kg/day of Isoproterenol hydrochloride (Iso) was inserted subcutaneously into each individual mouse and heart rate measured for an additional two weeks. Orally administered racemic carvedilol was dissolved in drinking water at an estimated dose of (32 mg/kg/day) for half the mice and 100  $\mu$ M of T-CAR gel (300  $\mu$ L) was applied topically to the other half every day. Due to the inherent variability in tail cuff data, the individual mouse heart rate data was averaged for the four sessions in each of the treatment paradigms as displayed in Fig. 6B. Two mice in the oral carvedilol group, and one mouse in the T-CAR group were excluded from the final analysis because the minipumps did not remain within the mice for the duration of the

study. Surprisingly, Iso treatment did not increase the heart rate of the SKH-1 mice. However, orally administered carvedilol, but not T-CAR, statistically reduced the heart rate ( $p < 0.000001$ ) (Fig. 6B). This study confirmed that topically applied T-CAR may have no effect on the cardiovascular system.

Twenty-four hours after the last T-CAR treatment, the drug level was analyzed in mouse plasma and skin. The data indicated that even at ten times the concentration of the single dose pharmacokinetics study (100  $\mu$ M) for multiple doses, the systemic absorption of drug from T-CAR was below our limit of quantification (Fig. 6C). The oral administration group had concentrations similar to those observed at the 8 h time point of the single-dose pharmacokinetic study. However, the skin tissue from these mice shows drastically different concentrations of carvedilol than the plasma. Topical T-CAR treatment showed statistically higher amount of drug in the skin tissues than mice treated with oral carvedilol, and significantly greater levels than found in the plasma (Fig. 6D). Furthermore, the oral carvedilol group had greater levels of carvedilol in the skin than found in the plasma, suggesting that the skin can act as a

**Table 1**  
Effects of T-CAR on the emergence and progression of UV-induced skin tumors.

Parameter	UV control	Empty	T-CAR	Statistics
Mice in experiment	10	10	10	
Total number of tumors <sup>a</sup>	34	25	21	
Tumors per mouse <sup>b</sup>	4 ± 2 <sup>a</sup>	3 ± 1 <sup>a</sup>	2 ± 1 <sup>b</sup>	RM-ANOVA: p = 0.0348
Tumor diameter (mm) <sup>c</sup>	48.2 ± 13.6 <sup>a</sup>	26.3 ± 7.5 <sup>a</sup>	10.6 ± 3.6 <sup>b</sup>	RM-ANOVA: p = 0.0221
Doubling Time (weeks) <sup>d</sup>	3.2 ± 2.4	3.0 ± 2.5	2.1 ± 2.0	ANOVA: p = 0.616
Median incidence week <sup>e</sup>	17 ± 1 <sup>a</sup>	16 ± 0 <sup>a</sup>	21 ± 3 <sup>b</sup>	ANOVA: p = 0.0364

<sup>a</sup> Tumors are counted as any mass having a diameter of at least 1 mm before sacrificing the mouse.

<sup>b</sup> Data expressed as median ± median absolute deviation (MAD) at 25 weeks; values with different Greek letters are statistically different as per a Kruskal-Wallis Multiple-Comparison Z-Value post hoc test. The repeated measures ANOVA statistic is provided and identified the same differences in the groups.

<sup>c</sup> Data expressed as mean ± SEM at 25 weeks; values with different Greek letters are statistically different as per a Tukey-Kramer Multiple-Comparison post hoc test. The repeated measures ANOVA statistic is provided and identified the same differences in the groups.

<sup>d</sup> Data expressed as mean ± SD; no statistical difference was identified in growth rates.

<sup>e</sup> Data expressed as median ± MAD; values with different Greek letters are statistically different as per a Kruskal-Wallis Multiple-Comparison Z-Value post hoc test.

reservoir for carvedilol similar to adipose tissue. These data further indicate that T-CAR at doses much lower than the oral dose (12 µg versus approximately 800 µg per mouse per day, respectively) provides a local

delivery of the drug to the skin without systemic absorption.

#### 4. Discussion

Although carvedilol is a safe drug for patients with cardiovascular conditions, its most pronounced effect is to slow the heart rate and thereby reduce cardiac output and blood pressure. The cardiovascular effects are a major obstacle for repurposing carvedilol as a cancer preventive agent. Another limitation for the use of carvedilol for skin cancer prevention is the delivery issue due to a significant degree of first-pass metabolism: the oral bioavailability is only ~ 24% (von Mollendorff et al., 1987). Thus, to accumulate carvedilol in the skin, high therapeutic doses are required. In practice, carvedilol is taken twice daily to maintain therapeutic concentrations. Topical drug delivery has demonstrated significant advantages in clinical practice for drugs targeting the skin, which avoids first-pass metabolism and reduces systemic side effects.

A transfersome® is a cutting-edge topical nano-delivery system for delivering drug into skin with diminished systemic effects (El Maghraby et al., 2001; Elsayed et al., 2007). Our previous study indicates that topical carvedilol loaded nano-transfersomes (T-CAR) produced a controlled and prolonged delivery of carvedilol to the skin (Chen et al., 2020b). The transfersomes generated for this project fit the desired size for penetrating the outer skin layer (Fig. 1) with high encapsulation efficiency (Supplementary Table 1), which is similar to previous reports (Chen et al., 2020b). The present study extended safety and efficacy experiments of T-CAR formulated with a Carbopol gel. The T-CAR gel was produced as it represents a viable formulation for human use. The new formulation necessitated repeating previous studies to determine if the formulation alters carvedilol-mediated pharmacokinetics and pharmacodynamics.

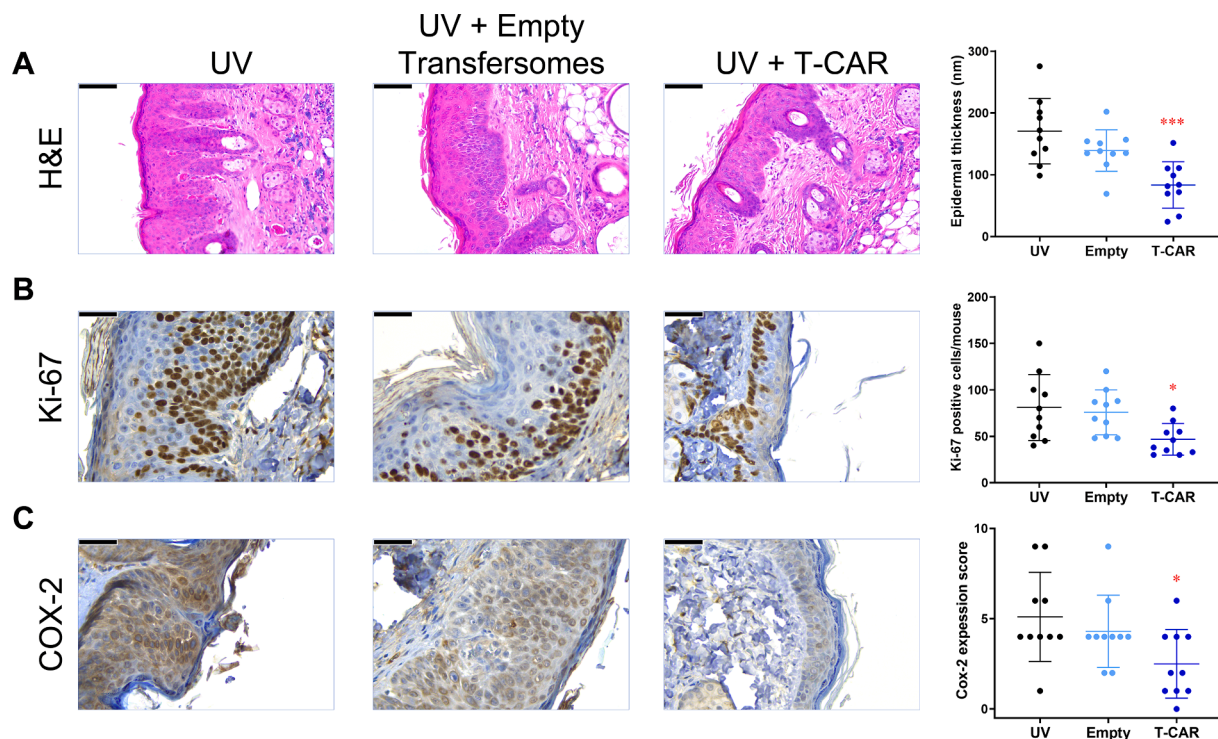


**Fig. 5.** Effects of T-CAR gel on UV-induced skin tumors and inflammation in the skin surrounding the tumors in SKH-1 mice. (A) Representative microphotographs of mouse skin stained with H&E. The thickness was measured five times at various locations along the epidermis and averaged to obtain a single skin samples data (n = 8). (B) Immunohistochemistry of Ki-67. Quantification of the number of Ki-67 positive cells (n = 8). (C) Immunohistochemistry of COX-2. The expression index was used to quantify the extent and intensity of COX-2 expression in each sample (n = 8). An ANOVA followed by a Tukey-Kramer multiple-comparison post hoc test was used to assess statistical differences at p < 0.05. All data are shown with the mean ± SD.

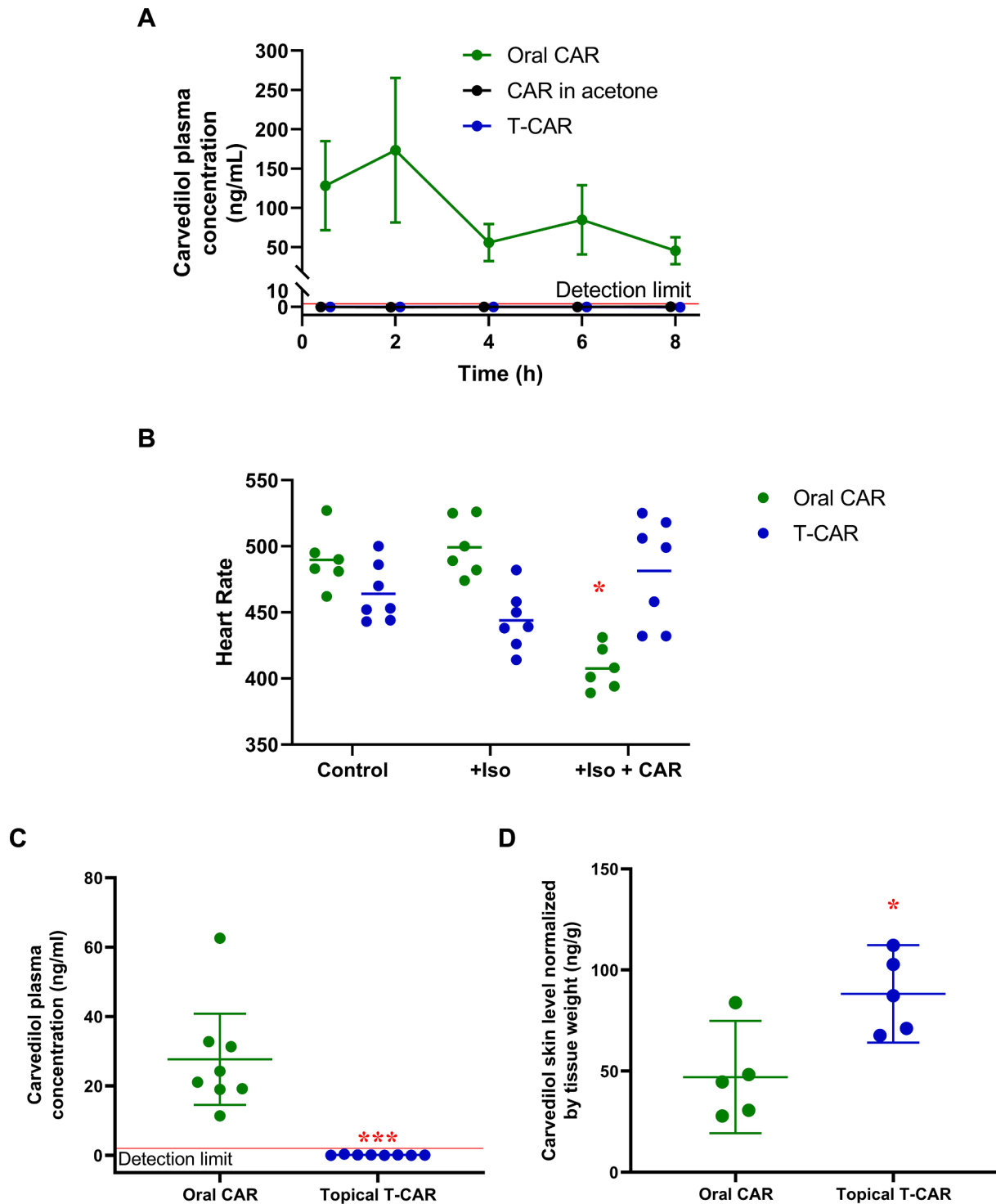


**Fig. 6.** Pharmacokinetic and cardiovascular analysis of T-CAR gel. (A) Plasma carvedilol (CAR) in mice treated with single dose topical T-CAR, CAR in acetone or oral gavage of 20 mg/kg CAR as a positive control. The detection limit is shown with a red line, and the data are offset to visualize the points ( $n = 3$ ). (B) Average heart rate was plotted and analyzed via a RM-ANOVA followed by Tukey-Kramer post hoc test to assess statistical differences at  $p < 0.05$  (\*).  $n = 6$  for the oral CAR group and  $n = 7$  for the T-CAR group; the line represents the group mean. Plasma (C) and skin (D) concentration of carvedilol in mice from the heart rate study; carvedilol treatments were 32 mg/kg oral carvedilol and 100  $\mu$ M T-CAR. Data is expressed as mean  $\pm$  95% CI, the detection limit is shown with a red line, and data were analyzed via *t*-test; \* =  $p < 0.05$  and \*\*\* =  $p < 0.001$ .

#### 4.1. Pharmacokinetic studies

The hypotheses regarding pharmacokinetics were that the T-CAR gel does not facilitate systemic delivery of carvedilol, and consequently would eliminate carvedilol-mediated cardiovascular effects. As shown in Fig. 2, there is no statistical difference between T-CAR suspension and T-

CAR gel in drug permeation through the skin or retention within the skin. Although short term UV studies are not pharmacokinetic in nature, an effect on CPD and skin thickness is observable (Fig. 3) suggesting that carvedilol is likely to be in the skin. Notably,  $3.4\% \pm 2.7\%$  of the T-CAR suspension and  $4.5\% \pm 3.4\%$  of the T-CAR gel transited the skin by 6 h (Fig. 2) supporting that T-CAR can get into the skin within 6 h. Future

studies will examine the percent of drug penetration into the mouse skin *in vivo* at different time points to gain a better understanding of the temporal nature of T-CAR gel skin deposition.

The *in vivo* pharmacokinetic data demonstrate that a single dose of oral carvedilol results in an elimination half-life of 4 to 7 h, which is consistent with human data (Morgan, 1994). However, T-CAR gel applied to the back of the mouse did not result in significant plasma concentrations of carvedilol in a single (Fig. 6A) or repeated dosing (Fig. 6C) studies. Conversely, T-CAR gel administration resulted in carvedilol accumulation within the skin (Fig. 6D). The skin accumulation data demonstrates T-CAR gel with a dose of carvedilol 66-fold less than the oral administration resulted in greater skin accumulation, confirming the effectiveness of the T-CAR delivery system. Surprisingly, the skin appears to be a sink for orally delivered carvedilol as the mean carvedilol values are greater than the plasma concentration; however, further studies are required as the analysis is underpowered. The presence of carvedilol within the skin suggests that retrospective medical record-based studies that have demonstrated an effect of carvedilol in reducing the occurrence and severity of multiple cancers (Gillis et al., 2021; Lin et al., 2015) should be conducted specifically to examine skin cancer incidence and severity.

The cardiovascular studies (Fig. 6B-D) utilized a 10-fold higher dose than the cancer studies (Fig. 4). The rationale for increasing the dose was to rigorously test the local deliverability of T-CAR. So far, the data suggest that T-CAR will be found safe after repeated administration. The pharmacokinetic data indicates that the T-CAR gel formulation and topical application prevent carvedilol from entering the systemic circulation. These conclusions are supported by the lack of any cardiovascular effects of T-CAR gel (Fig. 6B), discussed below.

#### 4.2. Pharmacodynamic studies

The hypotheses regarding pharmacodynamics were that 1) T-CAR gel will show similar skin cancer preventative properties to free carvedilol dissolved in acetone, 2) T-CAR gel will prevent UV-induced skin cancer, and 3) T-CAR gel will not decrease heart rate. The protective activity of T-CAR gel was firstly evaluated in SKH-1 mice exposed to single dose acute UV radiation (Fig. 3). The data indicate that the T-CAR gel and carvedilol dissolved in acetone create similar levels of protection against acute UV-induced epidermal thickening, which is primarily due to edema in the acute setting, and CPD formation. Although the mechanism of carvedilol-mediated chemoprevention remains unknown, the reduction in DNA damage likely plays a large role in the chemopreventive properties of carvedilol because it is known that accumulation of DNA damage results in skin carcinogenesis (Premi et al., 2015).

To confirm that the T-CAR gel formulation functions as a skin cancer preventative medication, long-term UV radiation experiments were conducted. The experimental design involves pretreatment of mice with test agents for two weeks, then exposing the mice to gradually increasing levels of UV radiation (50–150 mJ/cm<sup>2</sup>) three times a week for 25 weeks while giving treatment immediately after exposure to UV. Such UV exposure paradigms never result in sunburned skin and represents an accelerated model of the mechanism via which humans develop skin cancer. Therefore, the long-term UV exposure paradigm is an ideal preclinical test for efficacy of skin cancer preventative products. As shown in Fig. 4A and Table 1, T-CAR gel statistically attenuated tumor development indicating that the T-CAR gel formulation retains chemopreventive activity. The formulation itself had no effect. Expectedly the changes in tumor incidence are mirrored in the changes in tumor volume and multiplicity (Table 1). However, carvedilol does not alter the doubling time of the tumors. Classically, tumors are initiated (become a cancer) then progress (grow); the data suggest that carvedilol inhibits initiation but has no effect on progression. All the statistical differences in tumor number and size in the T-CAR group are due to carvedilol-induced delayed initiation followed by similar growth characteristics.

The excised tumors from the long-term study show greater severity in the UV and empty transference treatment groups compared to the T-CAR gel cohort (Fig. 4B). Furthermore, there is less epidermal thickening in non-tumorous skin (Fig. 5A). Epidermal thickening in the chronic UV study, unlike the acute studies, is likely due to hyperplasia as suggested by the Ki-67 and COX-2 staining seen in Fig. 5B & 5C, respectively. T-CAR gel reduced Ki-67 and COX-2 staining, further elucidating potential mechanisms of chemoprevention due to targeting of cell proliferation and inflammation. The data from Figs. 4 and 5 and Table 1 demonstrate that T-CAR gel prevents tumors and reduces measured pathological parameters in normal tissue, which fits the profile of a cancer preventative drug that blocks tumor initiation.

Although the long-term UV study demonstrates that carvedilol is an effective anti-cancer treatment (Huang et al., 2017b), there are caveats that must be explored prior to human trials. Imagining T-CAR gel as a product for human use brings one to the question of how it would be applied. Mice in an animal facility are not exposed to UV until the experimental paradigm; whereas humans are exposed to UV from early in life, whenever a human is in sunlight. Therefore, the idea of a long pre-treatment protocol is not applicable to expected human use. Two weeks pre-treatment, as shown in the pharmacokinetic studies (Fig. 6D), is sufficient to obtain a significant amount of carvedilol within the skin. It is unknown if the pretreatment paradigm is important to the result; moreover, it is not known when treatment should begin to obtain statistically meaningful cancer prevention. Therefore, future studies are required that alter the dose regimen to determine what is the minimal dosing required to reach a chemopreventive effect, and the maximal tolerated doses before adverse or cardiovascular effects are observed.

The cardiovascular studies demonstrate that daily T-CAR gel, at 10-fold greater concentrations than used for the cancer prevention studies, does not statistically alter heart rate (Fig. 6B); however, the cardiovascular experiment did not produce the expected data. The expectation is that T-CAR will not deliver appreciable amounts of carvedilol to the system circulation; therefore, the sympathetic system was activated via an osmotic minipump containing the  $\beta$ 1- and  $\beta$ 2-adrenergic receptors agonist Iso. However, the SKH-1 mice did not demonstrate the expected increase in heart rate following Iso exposure as reported for other mouse strains (Chang et al., 2018). Inspection of the data demonstrated that some mice responded better than others, and that 20  $\mu$ g Iso/kg/day increased heart rate, but not consistently in all mice. This suggests that the SKH-1 is not as responsive to Iso as other mice, which is not uncommon as the response to Iso is varied between mouse strains (Chang et al., 2018). Therefore, future studies will have to determine an appropriate dose of Iso to stimulate the  $\beta$ -adrenergic receptors prior to testing future cutaneous applications of carvedilol. Secondly, if SKH-1 mice are not as responsive to Iso, as other strains of mice, then they may not be as responsive to carvedilol, providing a false measure of T-CAR gel safety. In these studies, the pharmacokinetics indicates that plasma carvedilol is below our detection limit of 2 ng/mL; therefore, this study is unlikely a false measurement of no effect. However, the lack of effect of Iso demonstrates the need to test T-CAR adverse effects in multiple strains of mice, and select those that are more sensitive to Iso stimulation (Chang et al., 2018).

Due to the lack of Iso effect, the heart rate data was pooled over the four measurements per experimental condition. The pooling of data helped mitigate the variability in tail-cuff measurements; however, pooling data is not ideal as temporal effects are lost. Also, blood pressure was not specifically examined because Iso has a complicated blood pressure profile. Stimulation of  $\beta$ 1-adrenergic receptors leads to an increase in heart rate and stroke volume, but stimulation of vascular  $\beta$ 2-adrenergic receptors leads to vasodilation. This dual action can mitigate changes in blood pressure and makes analysis of the data complicated. However, as Iso failed to statistically influence heart rate we also saw no differences in blood pressure.

Taken together, our studies indicate that the novel T-CAR gel is able to deliver carvedilol into the skin without significant systemic

absorption. T-CAR gel, like the free drug treatment using acetone as a vehicle, prevents UV radiation induced skin damage, inflammation, and carcinogenesis in mice. These data provide essential evidence to support the feasibility of using nano-transfersome to deliver a highly potent  $\beta$ -blocker for photo-protection and skin cancer chemoprevention.

## Funding

Research reported in this publication was partly supported by the National Cancer Institute of the National Institutes of Health under Award Number R15CA227946 and Award Number R03CA256241 (Ying Huang). This work was also supported by Western University of Health Sciences Intramural Student Funds as part of the Graduate Program.

## CRedit authorship contribution statement

**Md Abdullah Shamim:** Data curation, Investigation, Writing – original draft. **Steven Yeung:** Methodology. **Ayaz Shahid:** Methodology. **Mengbing Chen:** Data curation, Investigation. **Jeffrey Wang:** Methodology. **Preshita Desai:** Methodology. **Cyrus Parsa:** Methodology. **Robert Orlando:** Methodology. **Frank L. Meyskens Jr:** Methodology. **Kristen M. Kelly:** Writing – review & editing. **Bradley T. Andresen:** Formal analysis. **Ying Huang:** Conceptualization, Funding acquisition, Supervision, Writing – review & editing.

## Declaration of Competing Interest

The authors declare that they have no known competing financial interests or personal relationships that could have appeared to influence the work reported in this paper.

## Acknowledgments

We thank Lily Kong Lim, A.S.C.P. (H.T.), at Beverly Hospital for preparing formalin-fixed paraffin-embedded tissues and H&E staining.

## Appendix A. Supplementary material

Supplementary data to this article can be found online at <https://doi.org/10.1016/j.ijpharm.2021.121302>.

## References

- Bhatia, A., Singh, B., Raza, K., Shukla, A., Amarji, B., Katare, O.P., 2012. Tamoxifen-loaded novel liposomal formulations: evaluation of anticancer activity on DMBA-TPA induced mouse skin carcinogenesis. *J. Drug Target* 20 (6), 544–550.
- Chang, A., Yeung, S., Thakkar, A., Huang, K.M., Liu, M.M., Kanassatega, R.S., Parsa, C., Orlando, R., Jackson, E.K., Andresen, B.T., Huang, Y., 2015. Prevention of skin carcinogenesis by the beta-blocker carvedilol. *Cancer Prev. Res (Phila)* 8, 27–36.
- Chang, S.C., Ren, S., Rau, C.D., Wang, J.J., 2018. Isoproterenol-Induced Heart Failure Mouse Model Using Osmotic Pump Implantation. *Methods Mol. Biol.* 1816, 207–220.
- Chen, M., Liang, S., Shahid, A., Andresen, B.T., Huang, Y., 2020a. The beta-Blocker Carvedilol Prevented Ultraviolet-Mediated Damage of Murine Epidermal Cells and 3D Human Reconstructed Skin. *Int. J. Mol. Sci.* 21.
- Chen, M., Shamim, M.A., Shahid, A., Yeung, S., Andresen, B.T., Wang, J., Nekkanti, V., Meyskens, F.L., Kelly, K.M., Huang, Y., 2020b. Topical Delivery of Carvedilol Loaded Nano-Transfersomes for Skin Cancer Chemoprevention. *Pharmaceutics* 12 (12), 1151. <https://doi.org/10.3390/pharmaceutics12121151>.
- Cleveland, K.H., Yeung, S., Huang, K.M., Liang, S., Andresen, B.T., Huang, Y., 2018. Phosphoproteome profiling provides insight into the mechanism of action for carvedilol-mediated cancer prevention. *Mol. Carcinog.* 57 (8), 997–1007.
- El Maghraby, G.M., Williams, A.C., Barry, B.W., 2001. Skin delivery of 5-fluorouracil from ultradeformable and standard liposomes in-vitro. *J Pharm Pharmacol* 53, 1069–1077.
- Elsayed, M.M., Abdallah, O.Y., Naggar, V.F., Khalafallah, N.M., 2007. Deformable liposomes and ethosomes as carriers for skin delivery of ketotifen. *Pharmazie* 62, 133–137.

- Freitas, J.V., Praça, F.S.G., Bentley, M.V.L.B., Gaspar, L.R., 2015. Trans-resveratrol and beta-carotene from sunscreens penetrate viable skin layers and reduce cutaneous penetration of UV-filters. *Int. J. Pharm.* 484 (1–2), 131–137.
- Gannu, R., Vishnu, Y.V., Kishan, V., Rao, Y.M., 2008. In vitro permeation of carvedilol through porcine skin: effect of vehicles and penetration enhancers. *PDA J. Pharm. Sci. Technol.* 62, 256–263.
- Gillis, R.D., Botteri, E., Chang, A., Ziegler, A.I., Chung, N.C., Pon, C.K., Shackelford, D.M., Andreassen, B.K., Halls, M.L., Baker, J.G., Sloan, E.K., 2021. Carvedilol blocks neural regulation of breast cancer progression in vivo and is associated with reduced breast cancer mortality in patients. *Eur. J. Cancer* 147, 106–116.
- Guy, G.P., Jr., Thomas, C.C., Thompson, T., Watson, M., Massetti, G.M., Richardson, L.C., Centers for Disease, C., Prevention, 2015. Vital signs: melanoma incidence and mortality trends and projections - United States, 1982-2030. *MMWR Morb Mortal Wkly Rep* 64, 591–596.
- Hanada, K., Asari, K., Saito, M., Kawana, J.-ichi, Mita, M., Ogata, H., 2008. Comparison of pharmacodynamics between carvedilol and metoprolol in rats with isoproterenol-induced cardiac hypertrophy: effects of carvedilol enantiomers. *Eur. J. Pharmacol.* 589 (1–3), 194–200.
- Huang, K.M., Liang, S., Yeung, S., Oiyemhonian, E., Cleveland, K.H., Parsa, C., Orlando, R., Meyskens, F.L., Jr., Andresen, B.T., Huang, Y., 2017a. Topically Applied Carvedilol Attenuates Solar Ultraviolet Radiation Induced Skin Carcinogenesis. *Cancer Prev Res (Phila)*.
- Huang, K.M., Liang, S., Yeung, S., Oiyemhonian, E., Cleveland, K.H., Parsa, C., Orlando, R., Meyskens, F.L., Andresen, B.T., Huang, Y., 2017b. Topically Applied Carvedilol Attenuates Solar Ultraviolet Radiation Induced Skin Carcinogenesis. *Cancer Prev Res (Phila)* 10 (10), 598–606.
- Jacobi, U., Kaiser, M., Toll, R., Mangelsdorf, S., Audring, H., Otberg, N., Sterry, W., Lademann, J., 2007. Porcine ear skin: an in vitro model for human skin. *Skin Res. Technol.* 13 (1), 19–24.
- Lademann, J., Jacobi, U., Surber, C., Weigmann, H.-J., Fluhr, J.W., 2009. The tape stripping procedure—evaluation of some critical parameters. *Eur. J. Pharm. Biopharm* 72 (2), 317–323.
- Liang, S., Shamim, M.A., Shahid, A., Chen, M., Cleveland, K.H., Parsa, C., Orlando, R., Andresen, B., Huang, Y., 2021. Prevention of skin carcinogenesis by the non-beta-blocking R-carvedilol enantiomer. *Cancer Prev Res (Phila)*.
- Lin, C.-S., Lin, W.-S., Lin, C.-L., Kao, C.-H., 2015. Carvedilol use is associated with reduced cancer risk: A nationwide population-based cohort study. *Int. J. Cardiol.* 184, 9–13.
- Ma, Z., Liu, X., Zhang, Q., Yu, Z., Gao, D., 2019. Carvedilol suppresses malignant proliferation of mammary epithelial cells through inhibition of the ROS-mediated PI3K/AKT signaling pathway. *Oncol. Rep.* 41, 811–818.
- Mahmood, S., Taher, M., Mandal, U.K., 2014. Experimental design and optimization of raloxifene hydrochloride loaded nanotransfersomes for transdermal application. *Int. J. Nanomed.* 9, 4331–4346.
- Morgan, T., 1994. Clinical pharmacokinetics and pharmacodynamics of carvedilol. *Clin. Pharmacokinet* 26 (5), 335–346.
- NTP, 2016. Report on Carcinogens, NTP (National Toxicology Program). Department of Health and Human Services, Public Health Service., Research Triangle Park, NC: U.S. Opatha, S.A.T., Titapiwatanakun, V., Chutoprapat, R., 2020. Transfersomes: A Promising Nanoencapsulation Technique for Transdermal Drug Delivery. *Pharmaceutics* 12 (9), 855. <https://doi.org/10.3390/pharmaceutics12090855>.
- Park, J., Kang, T., 2015. DNA Slot Blot Repair Assay. *Bio-protocol* 5, e1453.
- Premi, S., Wallisch, S., Mano, C.M., Weiner, A.B., Bacchicocchi, A., Wakamatsu, K., Bechara, E.J.H., Halaban, R., Douki, T., Brash, D.E., 2015. Photochemistry. Chemiexcitation of melanin derivatives induces DNA photoproducts long after UV exposure. *Science* 347 (6224), 842–847.
- Ricotti, C., Bouzari, N., Agadi, A., Cockerell, C.J., 2009. Malignant skin neoplasms. *Med. Clin. North America* 93 (6), 1241–1264.
- Rogers, H.W., Weinstock, M.A., Feldman, S.R., Coldiron, B.M., 2015. Incidence Estimate of Nonmelanoma Skin Cancer (Keratinocyte Carcinomas) in the US Population, 2012. *JAMA dermatology*.
- Sana, E., Zeeshan, M., Ain, Q.U., Khan, A.U., Hussain, I., Khan, S., Lepeltier, E., Ali, H., 2021. Topical delivery of curcumin-loaded transfersomes gel ameliorated rheumatoid arthritis by inhibiting NF-kappabeta pathway. *Nanomedicine (Lond)* 16, 819–837.
- Siegel, R.L., Miller, K.D., Jemal, A., 2019. Cancer statistics, 2019. *CA Cancer J. Clin.* 69 (1), 7–34.
- von Möllendorff, E., Reiff, K., Neugebauer, G., 1987. Pharmacokinetics and bioavailability of carvedilol, a vasodilating beta-blocker. *Eur. J. Clin. Pharmacol.* 33 (5), 511–513.
- Wang, J., Ono, K., Dickstein, D.L., Arrieta-Cruz, I., Zhao, W., Qian, X., Lamparello, A., Subnani, R., Ferruzzi, M., Pavlides, C., Ho, L., Hof, P.R., Teplow, D.B., Pasinetti, G. M., 2011. Carvedilol as a potential novel agent for the treatment of Alzheimer's disease. *Neurobiol. Aging* 32 (12), 2321.e1–2321.e12.
- Yao, A., Kohmoto, O., Oyama, T., Sugishita, Y., Shimizu, T., Harada, K., Matsui, H., Komuro, I., Nagai, R., Matsuo, H., Serizawa, T., Maruyama, T., Takahashi, T., 2003. Characteristic effects of alpha1-beta1,2-adrenergic blocking agent, carvedilol, on [Ca<sup>2+</sup>]<sub>i</sub> in ventricular myocytes compared with those of timolol and atenolol. *Circ. J.* 67 (1), 83–90.
- Zhang, G.X., Kimura, S., Nishiyama, A., Shokoji, T., Rahman, M., Yao, L., Nagai, Y., Fujisawa, Y., Miyatake, A., Abe, Y., 2005. Cardiac oxidative stress in acute and chronic isoproterenol-infused rats. *Cardiovasc. Res.* 65 (1), 230–238.